© 2013 ETRI

Retraction

This article has been retracted due to author misconduct. With the exception of two short paragraphs, “Double-Dwell Hybrid Acquisition in a DS-UWB System,” published in *ETRI Journal*, Vol. 29, No. 1, February 2007, pp. 1-7 is a duplicate of “Double-Dwell Hybrid Acquisition in DS-UWB System,” published in *The Journal of the Korean Institute of Communications and Information Sciences*, Vol. 31, No. 7A, 2006, pp. 696-701, article no. KICS2006-04-171.

Double submission and self-plagiarism are serious violations of publication policy and scholarship ethics. Upholding excellence in scholarship and maintaining the integrity of scientific information are the responsibilities of both authors and publishers. *ETRI Journal* takes any and all violations regarding authorship seriously, and each case of alleged misconduct is subject to a review by the editorial board.

Double-Dwell Hybrid Acquisition in a DS-UWB System

Yupeng Wang and KyungHi Chang

In this paper, we analyze the performance of double-dwell hybrid initial acquisition in a direct sequence ultra-wideband (DS-UWB) system via detection, miss, false alarm probabilities, and mean acquisition time. In the analysis, we consider the effect of the acquisition sequence as well as the deployment scenario of the abundant multipath components over small coverage of the piconet in the DS-UWB system. Based on the simulation, we obtain various performance measures for the mean acquisition time by varying parameters such as the total number of hypotheses to be searched, subgroup size, and dwell time. We thereupon suggest the optimum parameter set for the initial acquisition in the DS-UWB system.

Keywords: DS-UWB, hybrid acquisition, double-dwell.

RETRACTED

I. Introduction

Ultra-wideband (UWB) technology is the basis for wireless personal area networks (WPANs), intended for use on 3.1 to 10.6 GHz of unlicensed band, subject to the FCC Part 15 rules that specify a maximum transmit power spectral density of -41.3 dBm. UWB schemes can achieve very high aggregate data rates over short distances due to the ultra-wide bandwidths employed.

In a direct sequence UWB (DS-UWB) system, the goal of acquisition is to achieve the time alignment between the received spread code and the locally generated code to the accuracy of a fraction of one spread code chip. Unlike the conventional DS-CDMA system, acquisition is based on the acquisition sequence, not on the spread code itself.

One approach to achieving rapid acquisition is to use a double-dwell scheme rather than a single-dwell scheme [1], [2]. The advantage of the double-dwell scheme comes from the significant reduction of costly false alarms. A double-dwell scheme has two stages: search and verification. The former is used to make a tentative decision on the received code phase, and the latter is used to verify the decision in the search stage. To avoid increasing the correlation intervals for better reliability, verification methods based on multiple observations [2], [3] or differentially coherent combing [4] have been investigated. In multiple observation methods, a number of correlations are performed to obtain multiple observations for the cell under testing.

In this paper, we focus on the issues of initial acquisition in a DS-UWB system based on the acquisition sequence defined in the IEEE802.15.3a proposal [5] and the specific UWB channel model where abundant multipath components exist [6]. Compared with other studies, we obtain meaningful analytical results on initial acquisition, which are specific to the UWB channel environment in the presence of multiple H_1 hypotheses (in-phase cells) and data modulation in the acquisition sequence. We use the hybrid double-dwell scheme and divide the

Manuscript received Apr. 25, 2006; revised Oct. 26, 2006.
This work was supported by Inha University Research Grant.
Yupeng Wang (email: charles535@hotmail.com) and KyungHi Chang (phone: + 82 32 860 8422, email: khchang@inha.ac.kr) are with the Graduate School of Information Technology and Telecommunications, Inha University, Incheon, Korea.

hypotheses into several subgroups. The subgroup with H_1 hypotheses is called an H_1 subgroup. Otherwise, the subgroup with only H_0 hypotheses (out-phase cells) is called an H_0 subgroup. The simulation results for detection, miss, false alarm probabilities, and mean acquisition time are also presented under the UWB channel environment. Furthermore, we suggest the optimum dwell time and number of subgroups in search and verification modes based on the simulation results.

The remainder of this paper is organized as follows. In section II, we analyze a specific scenario in the UWB system and theoretically derive the detection, miss, and false alarm probabilities in search and verification modes. Also, we obtain the state transfer diagram and analytical mean acquisition time based on the above probabilities. All the analyses are conducted on the basis of a double-dwell hybrid acquisition scheme. We present the performance of initial acquisition in the DS-UWB system based on the acquisition sequence defined in the proposal and the double-dwell hybrid acquisition scheme in section III. Finally, conclusions are presented in section IV.

II. Analysis of Initial Acquisition Performance

1. Probability Distribution Function for DS-UWB System

With a large number of multipath components, the complex amplitude of the received signal has a complex Gaussian distribution [6]. Based on a non-coherent detector structure, the decision variable η, which is the sum of mutually-independent I/Q non-coherent correlator outputs Z_l, $l = 1, 2, \cdots, L$, is chi-squared distributed with $2L$ degrees of freedom under an H_0 or H_1 hypothesis [7]. The in-phase cell is denoted by H_1 and the out-phase cell is denoted by H_0. The probability density function of η under H_0 is

$$f_\eta(\eta|H_0) = \frac{1}{(L-1)!V_{H_o}^L}\eta^{L-1}e^{\frac{-\eta}{V_{H_0}}}, \quad (1)$$

where L is the post-detection integration period. Furthermore, we use V_{H_0} to represent the correlator output when the H_0 cell is under testing and $V_{H_0}=N_cI_0$. Here, N_c is the spreading factor of the acquisition sequence and I_0 is the interference spectral density which is caused by the background noise and other interference.

In this paper, we consider a multiple number of H_1 hypotheses. The probability density function of η under an H_1 hypothesis is given by

$$f_\eta(\eta|H_{1,i}) = \frac{1}{(L-1)!V_{H_{1,i}}^L}\eta^{L-1}e^{\frac{-\eta}{V_{H_{1,i}}}}, \quad i = 1,2,\cdots,I, \quad (2)$$

where $V_{H_{1,i}}$ refers to the output of the I/Q non-coherent correlator when the i-th H_1 hypothesis is under testing. In (3), $V_{H_{1,i}}$ is given by considering the effect of data modulation in the acquisition sequence:

$$V_{H_{1,i}} = N_c^2E_c\sum_{j=1}^{I} d^2(t)\cdot R_d^2(\lceil(\xi_i-\tau_j)/N_c\rceil) \cdot E[\alpha_j^2]\cdot R_c^2(\xi_i-\tau_j) + N_cI_0, \quad i = 1,2,\cdots,I. \quad (3)$$

Here, the acquisition sequence is generated in a manner in which a PN sequence is spread by the piconet acquisition code (PAC) [5]. In (3), E_c is the chip energy of PAC; $d(t)$ is the PN sequence to generate the acquisition sequence with a normalized autocorrelation function R_d, R_c is the normalized autocorrelation function of the PAC; and ξ_i and τ_j are the time information of the i-th H_1 hypothesis and the j-th path, respectively. Both time information values are normalized to one chip period T_c of the PAC.

According to the IEEE 802.15.SG3a final channel report [8], we have

$$\sum_{j=1}^{I} E[\alpha_j^2] = \sum \Omega_0 e^{-T_l/\Gamma}e^{-\tau_{k,l}/\gamma}, \quad (4)$$

where Ω_0 is the mean energy of the first path of the first cluster, T_l is the arrival time of the first path of the l-th cluster, and $\tau_{k,l}$ is the delay of the k-th path within the l-th cluster relative to the arrival time T_l of the first path. The cluster and ray decay factors are denoted by Γ and γ, respectively. For simplicity, we can convert (3) to (5) based on (4) with the assumption that the PN sequence used to generate the acquisition sequence is orthogonal.

$$V_{H_{1,i}} = N_c^2E_c\left(\sum \Omega_0 e^{-T_l/\Gamma}e^{-\tau_{k,l}/\gamma}\right)\left\{\sum_{j=1}^{I} R_c^2(\xi_i-\tau_j)\right\} + N_cI_0, \quad i = 1,2,\cdots,I, \quad (5)$$

where $|\xi_i - \tau_j| \le N_c$.

In the present work, we consider a hybrid acquisition scheme that combines both parallel acquisition and serial acquisition. The acquisition process consists of search and verification modes. The search and verification processes in the hybrid acquisition scheme are shown in Fig. 1, which consists of a bank of N parallel I/Q non-coherent correlators. The uncertainty region V, which is defined as the total hypotheses to be searched, is represented by W/Δ. Here, W denotes the maximum transmission delay according to the piconet coverage, and Δ represents the search step size. Both W and Δ are normalized to one chip period of the PAC.

We then partition the uncertainty region V into Q subgroups for the hybrid acquisition. Then, Q becomes V/M, where M is the number of hypotheses in one subgroup. In this paper, H_1

RETRACTED

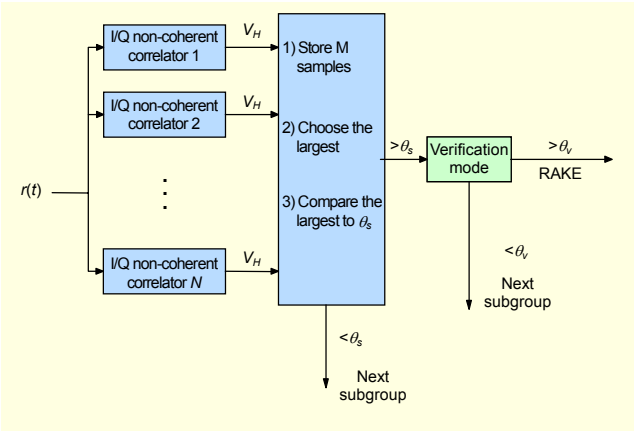

Fig. 1. Search and verification processing in hybrid acquisition scheme.

subgroup means the subgroup that contains at least one H_1hypothesis. However, the H_0 subgroup is that which contains no H_1 hypothesis.

Considering the deployment scenario of abundant multipath components over the small coverage of the piconet in a DS-UWB system, there is a much larger number of H_1 hypotheses compared with the conventional CDMA system. In addition, the multipath components are scattered over most of the uncertainty region under UWB channel environments; therefore, it is not practical to set the large subgroup size to contain all H_1 hypotheses in one or two subgroups as in the conventional CDMA system of [9]. In this paper, we assume n number of H_1 subgroups that contain H_1 hypotheses. The value of n depends on the number of H_1 hypotheses and the subgroup size M. We also assume that the i-th H_1 subgroup will contain I_i number of H_1 hypotheses.

2. Detection, Miss, and False Alarm Probabilities in Search and Verification Modes

In this section, using (1) to (5), we derive the detection, miss, and false alarm probabilities in both search and verification modes.

The detection probability $P^i_{d_{s,j}}$ in search mode for the j-th H_1 hypothesis in the i-th H_1 subgroup is defined in this paper as the probability that the correlation value at the j-th H_1 hypothesis is larger than the values at the other (M-1) hypotheses in the subgroup and the detection threshold θ_s of the search mode. We represent $P^i_{d_{s,j}}$ as

$$P^i_{d_{s,j}} = \int_{\theta_s}^{\infty} f_\eta(\eta|H_{1,j})\left[\int_0^{\eta} f_x(x|H_0)dx\right]^{M-I_i} \cdot \prod_{\substack{l=I_{i-1}+1 \\ l\neq j}}^{I_i}\left[\int_0^{\eta} f_y(y|H_{1,l})dy\right]d\eta, \quad (6)$$
$$i=1,2,\cdots,n,\ \ j=I_{i-1}+1,\cdots,I_i.$$

The detection probability $P^i_{d_s}$ in search mode for the i-th H_1 subgroup is then given as

$$P^i_{d_s} = \sum_{j=I_{i-1}+1}^{I_i} P^i_{d_{s,j}}, \qquad i=1,2,\cdots,n. \quad (7)$$

The miss probability $P^i_{m_s}$ in search mode for the i-th H_1 subgroup is defined as the probability that all the correlation values in the i-th H_1 subgroup are less than θ_s.

$$P^i_{m_s} = \prod_{j=I_{i-1}+1}^{I_i}\left[\int_0^{\theta_s} f_\eta(\eta|H_{1,j})d\eta\right]\left[\int_0^{\theta_s} f_\eta(\eta|H_0)d\eta\right]^{(M-I_i)} \quad (8)$$
$$i=1,2,\cdots,n$$

The false alarm probability $P^i_{f_s}$ in search mode for the i-th H_1 subgroup is given by

$$P^i_{f_s} = 1 - P^i_{d_s} - P^i_{m_s}, \qquad i=1,\ 2,\cdots,n. \quad (9)$$

The false alarm probability P_{f_0} in search mode for the H_0 subgroup is the probability that the correlation values at H_0 hypothesis exceed the detection threshold θ_s. It is given as

$$P_{f_0} = \left[\int_{\theta_s}^{\infty} f_\eta(\eta|H_0)d\eta\right]^M. \quad (10)$$

In verification mode, each hypothesis is tested independently without the concept of the subgroup. Hence, the detection probability $P_{d_{v,i}}$ of the verification mode is the probability that the correlation value at the H_1 hypothesis exceeds the detection threshold θ_v. It is represented as

$$P_{d_{v,i}} = \int_{\theta_v}^{\infty} f_\eta(\eta|H_{1,i})d\eta, \qquad i=1,2,\cdots,I. \quad (11)$$

The miss in verification mode means that a correlation value at the H_1 hypothesis is less than the detection threshold θ_v. The miss probability $P_{m_{v,i}}$ can be written as

$$P_{m_{v,i}} = \int_0^{\theta_v} f_\eta(\eta|H_{1,i})d_\eta, \qquad i=1,2,\cdots,I. \quad (12)$$

The false alarm probability P_{f_v} in verification mode means the probability that the correlation values at H_0 hypothesis exceed the detection threshold θ_v.

$$P_{f_v} = \int_{\theta_v}^{\infty} f_\eta(\eta|H_0)d\eta. \quad (13)$$

3. Analytical Mean Acquisition Time

The hybrid acquisition system described above can be represented as the state diagram shown in Fig. 2. In this figure, $H_0(z)$ denotes the state transfer function from the H_0 subgroup

RETRACTED

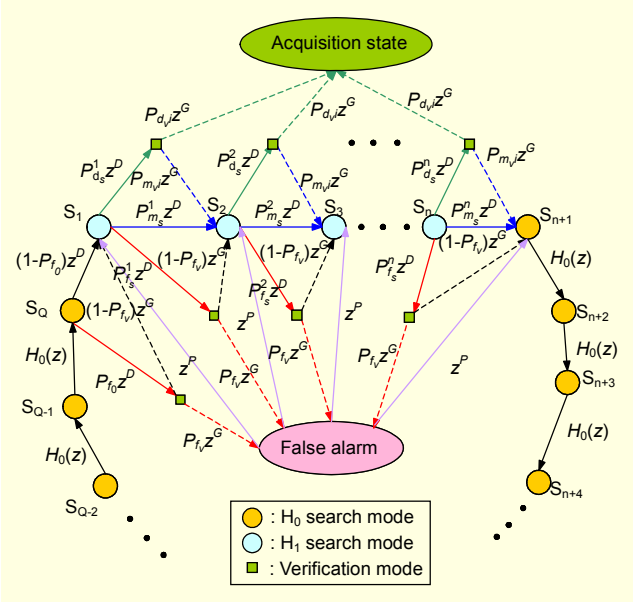

Fig. 2. State transfer diagram for hybrid scheme.

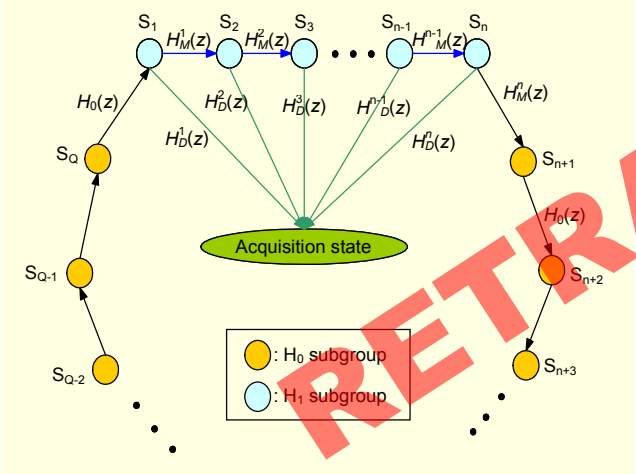

Fig. 3. Simplified state transfer diagram.

to the next subgroup, D is the number of hypotheses assigned to a correlator, G is the ratio of the dwell time in verification mode to the dwell time in search mode, and P is the penalty time when a false alarm occurs.

Figure 3 is the simplified state transfer diagram of Fig. 2. In Fig. 3, $H_D^i(z)$ represents the state transfer function that starts at the i-th H_1 subgroup and successfully ends at the acquisition state. The miss-state transfer function is denoted by $H_M^i(z)$, which proceeds from the i-th H_1 subgroup to the next subgroup. As shown in both Figs. 2 and 3, the system searches the subgroups in a clockwise direction. Referring to Figs. 2 and 3, we can obtain the state transfer function and finally derive the mean acquisition time (MAT) in theory.

Referring to Fig. 2, we have

$$H_D^i(z) = \sum_{j=I_{i-1}+1}^{I_i} P_{d_s,j}^i P_{d_v,j}, \quad i = 1,2,\cdots,n, \tag{14}$$

$$H_M^i(z) = P_{m_s}^i z^D + \sum_{j=I_{i-1}+1}^{I_i} P_{d_s,j}^i P_{m_v,j} z^{D+G} + P_{f_s}^i P_{f_v} z^{D+G+P} + P_{f_s}^i (1-P_{f_v}) z^{D+G}, \tag{15}$$

$$H_0(z) = (1-P_{f_0}) z^D + P_{f_0} P_{f_v} z^{D+G+P} + P_{f_0}(1-P_{f_v}) z^{D+G}. \tag{16}$$

In Fig. 3, the transfer function from an initial H_0 subgroup which is i branches counter-clockwise away from the first H_1 subgroup S_1 to the acquisition (ACQ) state is given by

$$T_i(z) = \frac{(H_0(z))^i H_D^1(z)}{1-(H_0(z))^{Q-n} \prod_{j=1}^{n} H_M^j(z)}. \tag{17}$$

The transfer function that starts at the k-th H_1 subgroup S_k is represented by

$$T_k(z) = \frac{H_D^k(z)}{1-(H_0(z))^{Q-n} \prod_{j=1}^{n} H_M^j(z)}. \tag{18}$$

From (17) and (18), since all subgroups are equally likely to be a priori, the resultant transfer function averaged over all Q starting subgroups is represented by

$$U(z) = \frac{1}{Q}\left[\sum_{i=1}^{Q-n} T_i(z) + \sum_{k=1}^{n} T_k(z)\right] = \frac{1}{Q} \frac{H_0(z)[1-(H_0(z)^{Q-n})] H_D^1(z) + [1-H_0(z)] \sum_{k=1}^{n} H_D^k(z)}{[1-H_0(z)][1-(H_0(z))^{Q-n} \prod_{j=1}^{n} H_M^j(z)]}. \tag{19}$$

Thus, the mean acquisition time is given by

$$\begin{aligned} E[T_{ACQ}] &= \frac{d}{dz} U(z)\Big|_{z=1} \cdot \tau_s \\ &= U(z) \frac{d}{dz} \ln U(z)\Big|_{z=1} \cdot \tau_s \\ &= U(z)[A(z) - B(z) - C(z)]\Big|_{z=1} \cdot \tau_s, \end{aligned} \tag{20}$$

where τ_s is the dwell time in search mode. The functions of $A(z)$, $B(z)$, and $C(z)$ are given in (21)-(23), where the prime sign ($'$) denotes the derivative on z.

RETRACTED

$$A(z) = \frac{\mathrm{NUM_A}}{\mathrm{DEN_A}}, \tag{21}$$

where

$$\begin{aligned}\mathrm{NUM_A} &= H_0'(z)H_D^1(z)[1-(H_0(z)^{Q-n})] \\ &\quad + H_0(z)H_D^{1\prime}(z)[1-(H_0(z)^{Q-n})] \\ &\quad + (n-Q)H_0(z)^{Q-n}H_0'(z)H_D^1(z) \\ &\quad + \sum_{k=1}^{n}[(1-H_0(z))H_D^{k\prime}(z) - H_0'(z)H_D^k(z)],\end{aligned}$$

$$\begin{aligned}\mathrm{DEN_A} &= H_0(z)[1-(H_0(z)^{Q-n})]H_D^1(z) \\ &\quad + [1-H_0(z)]\sum_{k=1}^{n}H_D^k(z).\end{aligned}$$

$$B(z) = -\frac{H_0'(z)}{1-H_0(z)}, \tag{22}$$

$$\begin{aligned}C(z) = &-\frac{(Q-n)(H_0(z))^{Q-n-1}H_0'(z)\prod_{j=1}^{n}H_M^j(z)}{1-(H_0(z))^{Q-n}\prod_{j=1}^{n}H_M^j(z)} \\ &+\frac{(H_0(z))^{Q-n}\sum_{j=1}^{n}[H_M^{j\prime}(z)\prod_{\substack{k=1\\k\neq j}}^{n}H_M^j(z)]}{1-(H_0(z))^{Q-n}\prod_{j=1}^{n}H_M^j(z)}.\end{aligned} \tag{23}$$

III. Validation of Initial Acquisition Performance

In this section, we validate the performance of initial acquisition via detection, miss, false alarm probabilities, and mean acquisition time based on the acquisition sequence in a DS-UWB system.

The parameters in the simulation are set as follows:

- Coverage of the piconet: 10 meters
- Fixed thresholds in search and verification modes
  - Threshold in search mode: 0.15
  - Threshold in verification mode: 0.20
- Acquisition sequence: nominal preamble structure defined in [5]
- Chip rate of PAC: 1.365 GHz
- Penalty time: 10^6 chip periods
- UWB channel model 1 with 100 channel realizations. Here, the number of multipath components is adapted to $NP_{10\mathrm{dB}}$ [8].

In Fig. 4, we present the probabilities of detection, miss, and false alarm for different cases of hypothesis number. According to the coverage of the piconet, we find that there are a total of 91 hypotheses with one-chip step size for search, that is, 182 hypotheses with half-chip step size. Furthermore, for cases in which the receiver is located at the boundary of the piconet, it is considered that some H_1 hypotheses might be out of the uncertainty region according to the multipath profile. Hence, we extend the uncertainty region up to 121 hypotheses so as to contain all existing H_1 hypotheses. From Fig. 4, after extension of the uncertainty region, we observe better detection and miss probabilities, while the false alarm probability is nearly the same. Comparing the cases of one-chip and half-chip search step size, we find that the probabilities of detection and miss with half-chip step size are much better. However, the false alarm probability with half-chip step size is worse for low E_b/N_0.

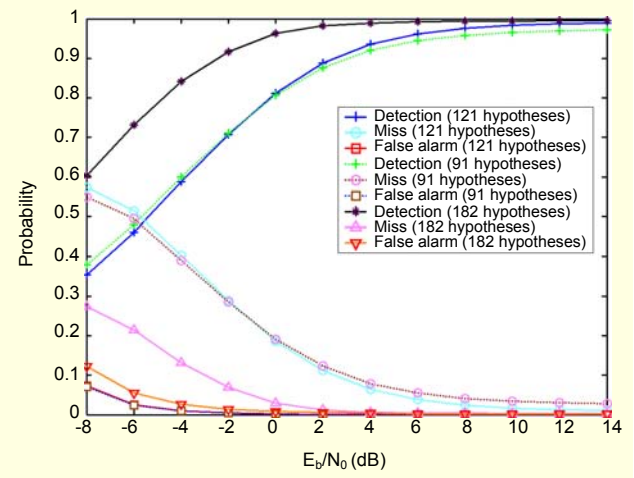

Fig. 4. Detection, miss, and false alarm probabilities. 1-chip step size for 91 and 121 hypotheses. 1/2-chip step size for 182 hypotheses.

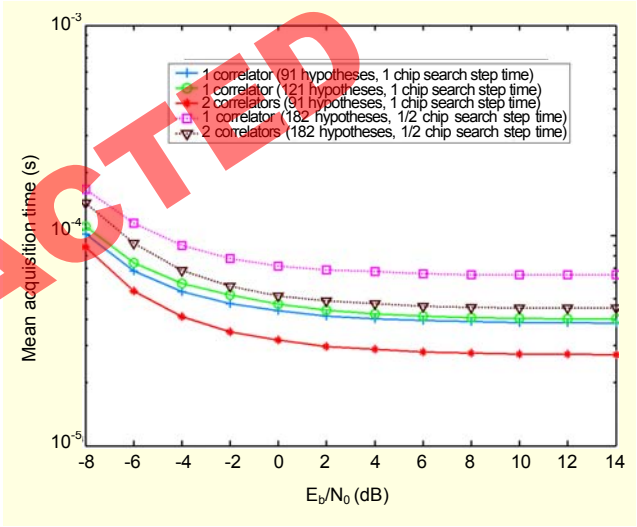

Fig. 5. Mean acquisition time under UWB channel model 1.

In Fig. 5, we show the performance of mean acquisition time for different cases of search step size, number of

RETRACTED

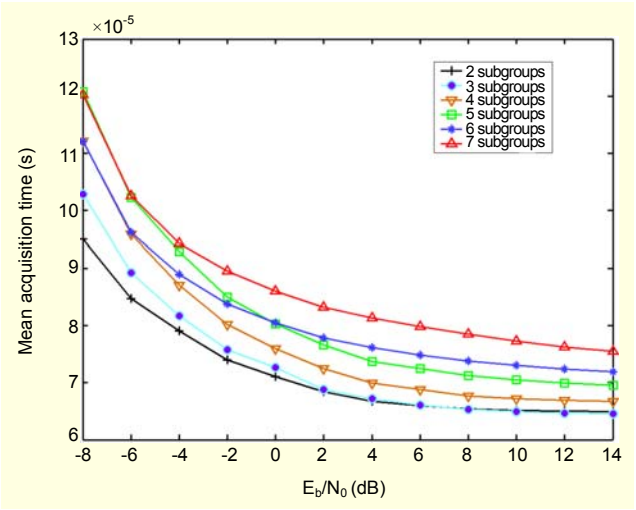

Fig. 6. Mean acquisition time with different number of subgroups under channel model 1.

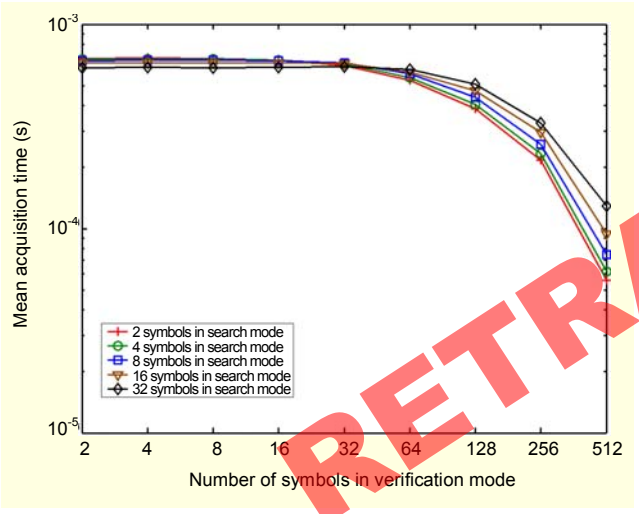

Fig. 7. MAT with the different dwell time in search and verification modes with -8 dB E_b/N_0 under channel model 1.

correlators, and uncertainty region. We see that the mean acquisition time is relative to the number of hypotheses. The larger the number of hypotheses, the longer the mean acquisition time. Mean acquisition time becomes longer when the uncertainty region is extended. Smaller step size and a decreased number of correlators also increase the mean acquisition time.

Figure 6 shows the MAT performance of the DS-UWB system when the hypotheses are divided into different numbers of subgroups. From the simulation results, we find that the MAT performance is similar when the hypotheses are divided into 2 or 3 subgroups. The optimum MAT performance is obtained when there are 2 or 3 subgroups depending on E_b/N_0, that is, one subgroup will cover an interval of 45 or 30 chips, respectively.

We assess the MAT performance by varying the dwell time for search and verification modes. From Fig. 7, we see that the minimum MAT is obtained when we use 2 symbols for search mode and 512 symbols for verification mode, that is, the whole length of the acquisition sequence.

IV. Conclusions

In this paper, we analyzed the detection, miss, and false alarm probabilities of the DS-UWB system in search and verification modes, as well as the mean acquisition time under the specific UWB channel model. We then validated the performance of initial acquisition in the DS-UWB system through simulations. An increase in the number of H_1 hypotheses will increase the detection probability and reduce the miss probability in both modes. On the other hand, an increase in the number of H_0 hypotheses will increase the false alarm probability. Although extension of the uncertainty region yielded better detection and miss probabilities, this improvement did not result in an improvement in the mean acquisition time due to the increased number of hypotheses. Hence, extension of the uncertainty region so as to contain all the H_1 hypotheses is not recommended. Based on the above comparison for MAT performance, we propose a subgroup size of 30 or 45 chips depending on E_b/N_0 and a dwell time of 2 and 512 symbols for search and verification modes, respectively.

RETRACTED

References

[1] M.K. Simon, J.K. Omura, R.A. Scholtz, and B.K. Levitt, *Spread Spectrum Communications Handbook*, McGraw-Hill, NY, 1994.

[2] A.J. Viterbi, *CDMA: Principles of Spread Spectrum Communication*, Addison-Wesley, New York, 1995.

[3] H.R. Park, "A Parallel Code Acquisition Technique for M-ary Orthogonal Signals in a Cellular CDMA System," *IEEE Trans. Veh. Technol,* vol. 49, Sep. 2000, pp. 2003-2012.

[4] O.S. Shin, and B.J. Kang, "Differentially Coherent Combining for Double-Dwell Code Acquisition in DS-CDMA Systems," *IEEE Trans. Commun,* vol. 51, July, 2003, pp. 1046-1050.

[5] R. Fisher, R. Kohno, M. McLaughlin, and M. Welborn, *DS-UWB Physical Layer Submission to 802.15 Task Group 3a*, IEEE P802.15-04/0137r4, Jan. 2005.

[6] A.F. Molisch and J.R. Foerster, "Channel Models for Ultrawideband Personal Area Networks," *IEEE Wireless Communications*, vol. 10, no. 6, Dec. 2003, pp. 14-21.

[7] A. Papoulis and S.U. Pillai, *Probability, Random Variables and Stochastic Process*, McGraw-Hill, NY, 2002.

[8] Jeff Forster, Sub-committee Chair, *Channel Modeling Sub-committee Report*, IEEE P802.15-02/490r1-SG3a, Feb. 2003.
[9] B.J. Kang, H.R. Park, and Y. Han, "Hybrid Acquisition in DS/CDMA Forward Link," *Proc. IEEE 47th VTC-Spring*, vol. 3, May 1997, pp. 2123-2127.

Yupeng Wang received the BS degree in communication engineering from Northeastern University, Shenyang, China, in 2004. He received the MS degree in the Graduate School of Information Technology and Telecommunications, Inha University, Incheon, Korea, in 2006. He is currently a PhD student at Inha University. His research interests include 3GPP LTE systems, radio resource management, MIMO techniques, and UWB.

KyungHi Chang received the BS and MS degrees in electronics engineering from Yonsei University, Seoul, Korea, in 1985 and 1987, respectively. He received his PhD degree in electrical engineering from Texas A&M University, College Station, Texas, in 1992. From 1989 to 1990, he was with the Samsung Advanced Institute of Technology (SAIT) as a Member of Research Staff and was involved in digital signal processing system design. From 1992 to 2003, he was with the Electronics and Telecommunications Research Institute (ETRI) as a Principal Member of Technical Staff. During this period, he led the team of WCDMA UE modem design and 4G radio transmission technology (RTT). He is currently with the Graduate School of Information Technology and Telecommunications, Inha University, where he has been an Associate Professor since 2003. His current research interests include RTT design for IMT-Advanced & 3GPP LTE systems, WMAN system design, cognitive radio, cross-layer design, and cooperative relaying system. Dr. Chang has served as a Senior Member of IEEE since 1998. Currently he is an Editor in Chief for the Korean Institute of Communication Sciences (KICS) Proceedings. He has also served as an Editor of ITU-R TG8/1 IMT.MOD, and he is currently an International IT Standardization Expert of Telecommunications Technology Association (TTA).

RETRACTED